BIOCHEMISTRY
including biophysical chemistry & molecular biology

Article

pubs.acs.org/biochemistry

Near-UV Circular Dichroism and UV Resonance Raman Spectra of Individual Tryptophan Residues in Human Hemoglobin and Their Changes upon the Quaternary Structure Transition

Masako Nagai,*[,†] Shigenori Nagatomo,[‡] Yukifumi Nagai,[†] Kenichi Ohkubo,[§] Kiyohiro Imai,[§] and Teizo Kitagawa*[,⊥]

[†]Research Center for Micro-Nano Technology, Hosei University, Koganei, Tokyo 184-0003, Japan

[‡]Department of Chemistry, University of Tsukuba, Tsukuba, Ibaraki 305-8571, Japan

[§]Department of Frontier Bioscience, Faculty of Bioscience and Applied Chemistry, Hosei University, Koganei, Tokyo 184-8584, Japan

[⊥]Picobiology Institute, Graduate School of Life Science, University of Hyogo, 3-2-1, Kouto, Kamigori, Ako-gun, Hyogo 678-1297, Japan

Supporting Information

ABSTRACT: The aromatic residues such as tryptophan (Trp) and tyrosine (Tyr) in human adult hemoglobin (Hb A) are known to contribute to near-UV circular dichroism (CD) and UV resonance Raman (RR) spectral changes upon the R → T quaternary structure transition. In Hb A, there are three Trp residues per $\alpha\beta$ dimer: at α14, β15, and β37. To evaluate their individual contributions to the R → T spectral changes, we produced three mutant hemoglobins in *E. coli*; rHb (α14Trp→Leu), rHb (β15Trp→Leu), and rHb (β37Trp→His). Near-UV CD and UVRR spectra of these mutant Hbs were compared with those of Hb A under solvent conditions where mutant rHbs exhibited significant cooperativity in oxygen binding. Near-UV CD and UVRR spectra for individual Trp residues were extracted by the difference calculations between Hb A and the mutants. α14 and β15Trp exhibited negative CD bands in both oxy- and deoxy-Hb A, whereas β37Trp showed positive CD bands in oxy-Hb A but decreased intensity in deoxy-form. These differences in CD spectra among the three Trp residues in Hb A were ascribed to surrounding hydrophobicity by examining the spectral changes of a model compound of Trp, *N*-acetyl-L-Trp ethyl ester, in various solvents. Intensity enhancement of Trp UVRR bands upon the R → T transition was ascribed mostly to the hydrogen-bond formation of β37Trp in deoxy-Hb A because similar UVRR spectral changes were detected with *N*-acetyl-L-Trp ethyl ester upon addition of a hydrogen-bond acceptor.

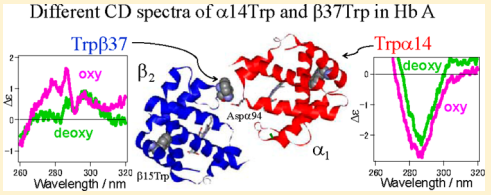

Human adult hemoglobin (Hb A) is composed of two α (141 residues) and two β (146 residues) subunits forming an $\alpha_2\beta_2$ tetramer. X-ray crystallographic studies of Hb A have demonstrated the presence of two distinct quaternary structures that correspond to low-affinity (tense or T) and high-affinity (relaxed or R) states, which have practically been determined for the unliganded form (deoxy-Hb) and ligand-bound form (CO- or oxy-Hb), respectively.[1,2] Aromatic residues such as tryptophan (Trp) and tyrosine (Tyr) are known to be involved in the R → T quaternary structure changes. The ^{1}H NMR signal of α42Tyr, which is hydrogen-bonded with β99Asp in the T form but free in the R form, serves as a practical marker of the quaternary structure in solution.[3]

As initially pointed out by Simon and Cantor,[4] near-UV circular dichroism (CD) spectra of Hb A at around the 285 nm region exhibit a characteristic change from a small positive band to a definite negative band upon the oxy (R) → deoxy (T) transition. It was later shown that this difference was not due to tertiary structure change by ligand binding but to environmental alterations around aromatic residues by quaternary structure transition, specifically by hydrogen-bond formation of α42Tyr and/or β37Trp upon deoxygenation.[5] The contribution of the aromatic residues to the negative CD band has been elucidated in detail,[6,7] but the nature of the environmental alteration is still unsolved. UVRR spectroscopy is a unique technique for selectively observing the vibrational spectra of Trp and Tyr residues and has revealed that quaternary structure transition brought about intensity enhancement of β37Trp residue.[8−13] However, the origin of this enhancement also remains to be specified.

There are three Trp residues per $\alpha\beta$ dimer of Hb A: at α14, β15, and β37. Trp residues occupy important positions of Hb molecule. α14Trp and β15Trp are located in the α1−β1 subunit interface, and β37Trp is located in the α1−β2 interface.[14] Crystal structures of Hb A have revealed that the N_1H proton of the indole ring of α14Trp forms a hydrogen bond with the hydroxyl group of α67Thr and that a similar hydrogen bond is formed between β15Trp and β72Ser. These

Received: March 15, 2012
Revised: June 20, 2012
Published: July 6, 2012

dx.doi.org/10.1021/bi300347x | *Biochemistry* 2012, 51, 5932−5941

two hydrogen bonds are thought to be vital for tertiary structure of Hb molecule by connecting A with E helices within the α and β chains, respectively. β37Trp is located in the C-helix corner, the "hinge region", of the $\alpha1-\beta2$ subunit interface. β37Trp interacts with α92Arg, α94Asp, and α95Pro of the FG corner of α-chain and with α140Tyr of the carboxyl terminus.[14,15] β37Trp makes an intersubunit hydrogen bond with α94Asp only in the deoxy-form.[16] Previous studies have shown that amino acid substitutions of β37Trp can result in significant increase of the tetramer-to-dimer dissociation in both the deoxy and oxy states of mutant Hbs.[14] In this way, the three Trp residues are placed at important positions of a Hb molecule and believed to play a vital role in the structure–function relationship of Hb A. β37Trp is placed in the subunit interface and makes an intersubunit hydrogen bond with α94Asp only in the deoxy-form.[16] To elucidate the individual contributions from three Trp residues to the negative CD band and intensity enhancement in UVRR spectra, we produced three mutant hemoglobins in *E. coli* using a site-directed mutagenesis[17] in which a nonaromatic residue is substituted for each Trp residue—rHb (α14Trp→Leu) (αW14L), rHb (β15Trp→Leu) (βW15L), and rHb (β37Trp→His) (βW37H)—and examined the nature of environmental alteration by comparing the spectra of each Trp residue extracted by the HbA-minus mutantHbs difference calculations with spectral changes of Trp model compounds in various solvents with or without a hydrogen-bond acceptor.

EXPERIMENTAL PROCEDURES

Hemoglobins. Hb A was purified from human hemolysate by preparative isoelectric focusing.[11] Mutant hemoglobins were prepared by a site-directed mutagenesis in *E. coli*. The Hb A expression plasmid, pHE7,[17] containing human α- and β-globin genes and the *E. coli* methionine aminopeptidase gene, was kindly provided by Professor Chien Ho of Carnegie Mellon University. Plasmids for rHb(αW14L), rHb(βW15L), and rHb(βW37H) were produced using an amplification procedure for closed circular DNA *in vitro*[18] and transformed into *E. coli* JM109. *E. coli* cells harboring the plasmid were grown at 30 °C in a TB medium.[17] Expression of recombinant hemoglobin (rHb) was induced by adding isopropyl β-thiogalactopyranoside. The culture was then supplemented with hemin (30 μg/mL) and glucose (15 g/L), and the growth was continued for 5 h at 32 °C. The cells were harvested by centrifugation and stored under frozen conditions at −80 °C until needed for purification. Recombinant Hbs were purified according to the methods described before.[19]

Reagents. *N*-Acetyl-L-tryptophan ethyl ester (Nac-L-Trp EE) (Aldrich), indole-3-methyl (skatole) and indole-3-acetic acid (Wako), indole-3-pyruvic acid (Sigma), and hexamethylphosphoric triamide (HMPA) (MP Biomedicals) were used as purchased.

Oxygen Equilibrium Experiments. Oxygen equilibrium curves were determined by using an automatic oxygenation apparatus.[20,21] The spectrophotometer used for the apparatus was a model U-4000 (Hitachi, Tokyo). Oxygen saturation was monitored as absorbance changes detected at 560 nm. Oxygen affinity (p_{50}) and cooperativity (Hill coefficient, n) were calculated from the best-fit stepwise Adair constants[21] that were determined from the equilibrium curve by a nonlinear least-squares method.[22] The hemoglobin concentration was 60 μM on a heme basis. The buffer used was a 0.05 M bis-Tris buffer (pH 7.4) containing 0.1 M Cl^-. The temperature within the oxygenation cell was maintained at 25.0 ± 0.1 °C. To minimize the autoxidation of hemoglobin during measurement, an enzymatic metHb reducing system[23] together with catalase and superoxide dismutase[24,25] were added to each sample. The amount of autooxidized Hb (metHb) after oxygen equilibrium measurement ranged from 0.9 to 5.5% of the total Hb.

CD Measurements. The measurements were carried out with a Jasco J-820 spectropolarimeter at 25 °C using a (+)-10-camphorsulfonic acid calibration. Absorption spectra were measured with a double-beam spectrophotometer (Hitachi, model U-3010).

UVRR Measurements. *235 nm Excitation.* UVRR spectra were excited by a XeCl excimer laser-pumped dye laser (Lambda Physik, model LPX120i and SCANMATE). The 308 nm line from the XeCl excimer laser (operated at 100 Hz) was used to excite coumarin 480, and the 470 nm output from the dye laser was frequency-doubled with a β-BaB_2O_4 crystal to generate 235 nm pulses. The Raman excitation light (3–4 mJ/cm^2) was introduced into samples from the lower front side of a spinning cell. The scattered light was dispersed with an asymmetric double monochromator (Spex 1404) in which the gratings in the first and second dispersion steps are 2400 grooves/mm (holographic) and 1200 grooves/mm (machine-ruled, 500 nm blaze), respectively, and was detected by an intensified photodiode array (Hamamatsu Photonics, model PCIMD/C5222-0110G).[11]

The spinning cell was moved vertically by 1 mm for every spectrum (every 5 min) to shift the laser illumination spot on the sample. Temperature of the sample solution was kept at 10 °C by flushing with cooled N_2 gas against the cell. The scattered light was collected with Cassegranian optics with f/1.1. One spectrum is composed of the sum of 400 exposures, each exposure accumulating the data for 0.8 s. All samples contained a common amount of sulfate ions, which yielded a band at 981 cm^{-1}. This band was used as an internal intensity standard for the normalization of Raman spectra.[26] Raman shifts were calibrated with cyclohexane. The integrity of the sample after exposure to the UV laser light was carefully confirmed by the visible absorption spectra measured before and after the UVRR measurements. If some spectral changes were recognized, the Raman spectra were discarded. Visible absorption spectra were recorded with a Hitachi 220S spectrophotometer.

229 nm Excitation. The excitation light at 229 nm (0.5 mW), which was obtained from an intracavity frequency-doubled Ar^+ ion laser (Coherent, Innova 300C FRED), was introduced onto a sample from the lower front side of the spinning cell, which was a quartz NMR tube (Wilmad-LabGlass, 535-PP-9SUP, diameter = 5 mm). The cell was spun using a hollow axis motor (Oriental Motor, BLU220A-5FR) at 160 rpm. The scattered light was collected and focused by two achromatic doublet lenses onto the entrance slit of a prism prefilter polychromator (Bunkoh-Keiki) to reject Rayleigh scattering. The prefilter was coupled to a 1 m single spectrograph (HORIBA Jobin Yvon, 1000M), equipped with a 200 nm blazed holographic grating with 3600 grooves/mm. A 135° backscattering geometry was adopted. The dispersed light was detected with a UV-coated, liquid-nitrogen-cooled CCD detector (Roper Scientific, Spec10:400B/LN). Each spectrum is the sum of 60 exposures, each exposure accumulating data for 30 s. Raman shifts were calibrated with cyclohexane as a frequency standard, and the frequency accuracy was ±1 cm^{-1}

dx.doi.org/10.1021/bi300347x | *Biochemistry* 2012, 51, 5932–5941

for well-defined Raman bands. Other procedures are common to those for 235 nm excitation.

RESULTS AND DISCUSSION

Oxygen Binding Properties of Three Mutant Hemoglobins. We expressed three mutant Hbs in *E. coli* and examined the effects of mutation on oxygen binding properties. As shown in Figure 1 and Table 1, rHb(αW14L) and rHb(βW15L) exhibited slightly increased oxygen affinity and significant cooperativity (Hill's n = 2.2−2.4) and stayed in a tetrameric form.[27] In contrast, rHb(βW37H) was dissociated into dimers in oxy-form and showed markedly increased oxygen affinity and low cooperativity (n = 1.8). In the presence of inositol hexaphosphate (IHP), however, rHb(βW37H) was stabilized as a tetramer and exhibited significant cooperativity (n = 2.1).[27] We measured the near-UV CD and UVRR spectra of these mutant rHbs which stayed as tetramers and exhibited significant cooperativity under the conditions shown in Table 1.

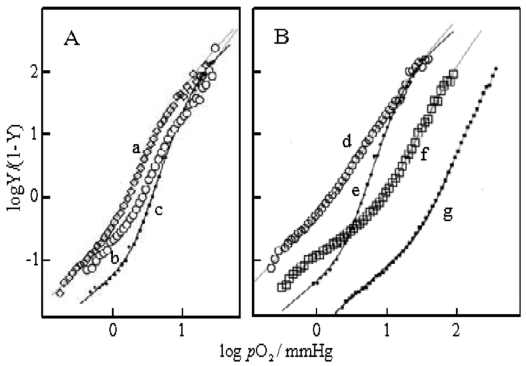

Figure 1. Hill's plots of oxygen binding by rHb(αW14L) (A-a), rHb(βW15L) (A-b), and rHb(βW37H) in the absence (B-d) and presence (B-f) of IHP compared with that of Hb A (−IHP) (A-c, B-e) and Hb A (+IHP) (B-g). Y is the fractional oxygen saturation, and pO_2 is the partial pressure of oxygen in mmHg. The symbols are observed points, and lines were calculated from the best-fit values of the four stepwise Adair constants.[21,22] The hemoglobin concentration was 60 μM on a heme basis in 0.05 M bis-Tris buffer (pH 7.4) containing 0.1 M Cl^-, and the temperature was at 25 °C. IHP was added to a final concentration of 2 mM.

Table 1. OEC Parameters and Dimer−Tetramer Assembly of Mutant Hemoglobins[a]

Hb	oxygen affinity (p_{50}, mmHg)	cooperativity Hill's n	dimer−tetramer assembly
rHb(αW14L)[b]	3.3	2.2	tetramer
rHb(βW15L)[b]	2.0	2.4	tetramer
rHb(βW37H) (−IHP)	1.6	1.8	dimer
rHb(βW37H) (+IHP)[b]	9.6	2.1	tetramer
Hb A (−IHP)[b]	4.2	2.8	tetramer
Hb A (+IHP)	46	2.3	tetramer

[a]OEC curves were examined using an automatic oxygenation apparatus in a 0.05 M bis-Tris buffer, pH 7.4, containing 0.1 M Cl^- at 25 °C. Oxygen affinity (p_{50}) and cooperativity (Hill's n) were calculated from the best-fit stepwise Adair constants that were evaluated from the curves of Figure 1.[20,21] Dimer−tetramer assembly of hemoglobins was determined by Sephadex G75 column chromatography and analytical ultracentrifugation.[27] [b]Experimental conditions used for CD and UVRR measurements.

Near-UV CD Spectra of Mutant Hemoglobins. Figure 2 shows the near-UV CD spectra of oxy-, deoxy-Hb A, and their difference (inset). Hb A exhibited two CD bands at 260 and 285 nm.

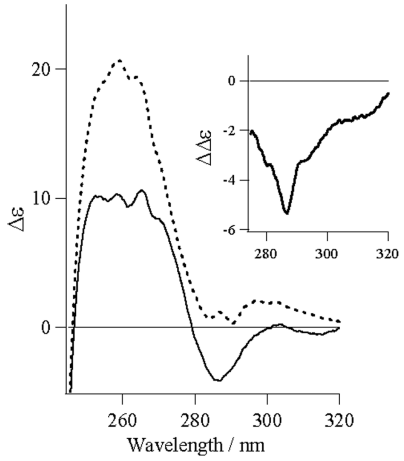

Figure 2. CD spectra of deoxy-form (solid line) and oxy-form (dotted line) of Hb A, and the deoxy-minus-oxy difference spectrum (inset). Hb, 50 μM (in heme) in a 0.05 M phosphate buffer (pH 7) was measured in a cell having a 2 mm light path length at 25 °C. The scan speed was 20 nm/min, and 40 scans were averaged.

The positive CD band at 260 nm is thought to derive from the heme moiety and is sensitive to the coordination and spin state of the heme. On the other hand, the band at 285 nm derives from aromatic residues such as Trp and Tyr in globin and changed upon oxygen binding (see inset), reflecting conformational transition.[4,5,28] To examine whether all three Trp residues in Hb A contribute to this CD band at 285 nm or not, we compared the CD spectra of three mutant hemoglobins—rHb(αW14L), rHb(βW15L), and rHb(βW37H)—with that of Hb A. Figure 3 shows the deoxy-minus-oxy difference spectra of these three mutants (green spectra) and Hb A (black spectra). Two recombinant Hbs, rHb(αW14L) and rHb(βW15L), showed difference spectra similar to that of Hb A, indicating that α14Trp and β15Trp did not significantly contribute to the negative CD band of deoxy-Hb A. On the other hand, rHb(βW37H) exhibited a smaller negative CD band than that of Hb A. As previously reported, β37Trp is partly responsible for the negative CD band of deoxy-Hb A.[6,7]

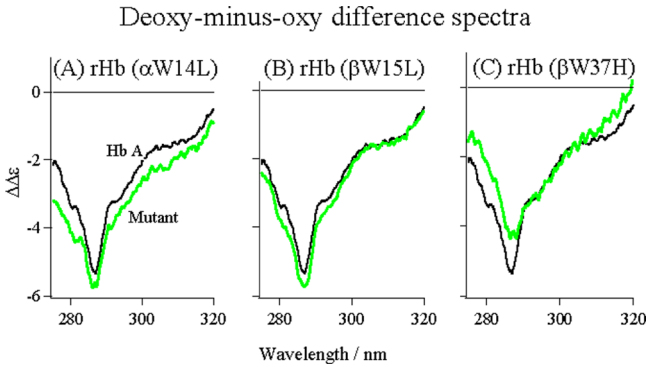

Figure 3. Comparison of the deoxy-minus-oxy difference CD spectra of rHb(αW14L), rHb(βW15L), and rHb(βW37H) (green spectra) with that of Hb A (black spectra). The experimental conditions were the same as those in Figure 2.

dx.doi.org/10.1021/bi300347x | *Biochemistry* 2012, 51, 5932−5941

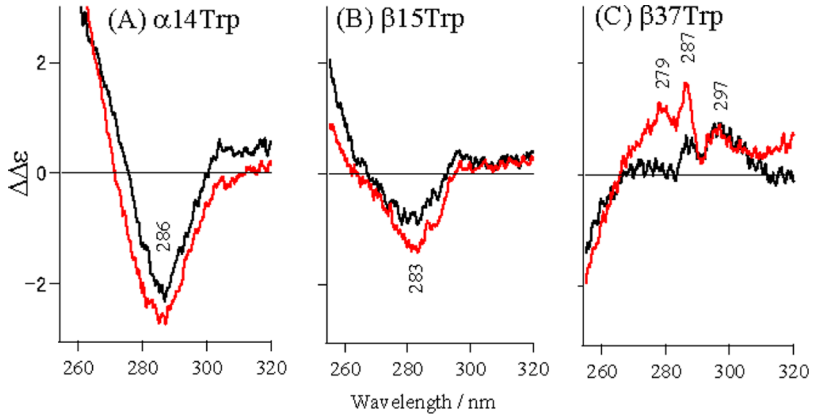

Figure 4. Difference spectra between Hb A and rHb(αW14L), rHb(βW15L), and rHb(βW37H) in the oxy-form (red spectra) and the deoxy-form (black spectra). The experimental conditions were the same as those described in the legend of Figure 2. These difference spectra were thought to reflect each Trp residue in Hb A.

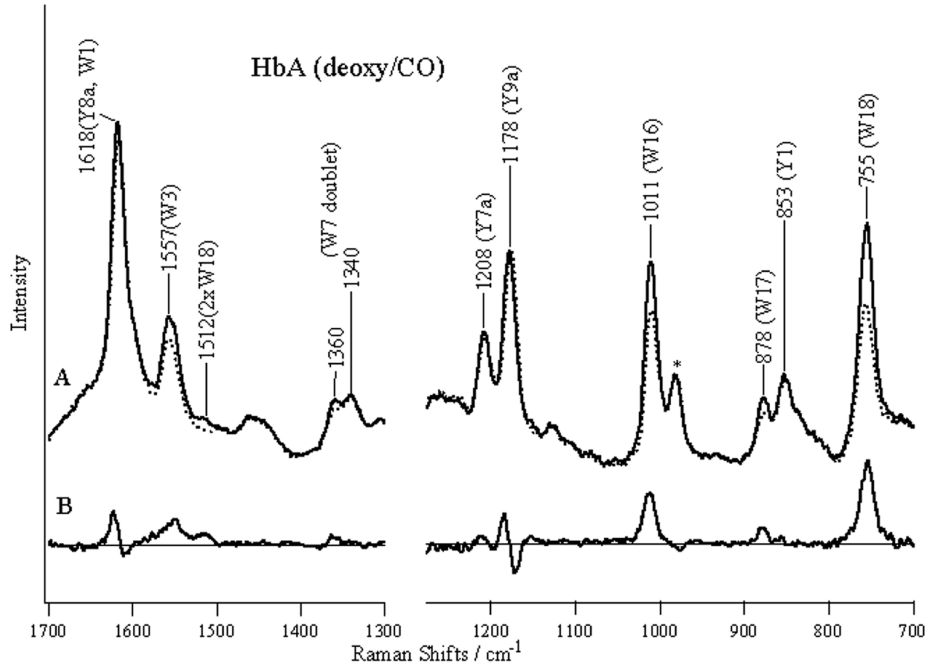

Figure 5. The 235 nm excited UVRR spectra of deoxy-Hb A (A: solid line), CO-Hb A (A: dotted line), and the difference between them (deoxy − CO) (B). The hemoglobin concentration was 400 μM (in heme) in a 0.05 M phosphate buffer (pH 7) containing 0.2 M SO_4^{2-} as the internal intensity standard. The difference spectrum was obtained so that the Raman band of SO_4^{2-} (marked by an asterisk) could be abolished. Each spectrum is an average of 20 scans.

The CD spectra of individual Trp residues were extracted by difference calculations, the Hb A-minus-individual mutant Hb. Figure 4 shows the CD spectra of individual Trp residues in both the oxy-form (red spectra) and deoxy-form (black spectra). A negative CD band appeared in both the oxy- and deoxy-forms at 286 nm for α14Trp and at 283 nm for β15Trp, and their negative intensities decreased appreciably in the deoxy-form compared to the oxy-form, supporting the possibility that these two Trp residues did not contribute to the deoxy-minus-oxy difference peak of Hb A shown in Figure 3. In contrast, β37Trp showed positive CD bands at 279, 287, and 297 nm in the oxy-form, and the first two bands decreased in intensity in the deoxy-form but the last band remained unchanged. Thus, it became evident that the negative CD peak at 286 nm in the deoxy-minus-oxy difference spectrum of Hb A arose from β37Trp. Although we previously proposed that the negative CD band at 286 nm of deoxy-Hb A, which has been used as the T-state marker, was mainly due to the penultimate Tyr of both the α and β subunits,[6,7] we modified it to that β37Trp also contributes to the negative CD band in addition to those Tyr residues.

The 235 nm Excited UV Resonance Raman Spectra of Mutant Hemoglobins. Figure 5 shows the 235 nm excited UVRR spectrum of deoxy- and CO-forms of Hb A (A) and its deoxy-minus-CO difference spectrum (B). The two spectra in Figure 5A are normalized with a band of SO_4^{2-} at 981 cm^{-1}. The raw spectrum of Hb A is dominated by the bands arising from three Trp and six Tyr residues per $\alpha\beta$ dimer, which are labeled W and Y, respectively, followed by their mode numbers.[29,30] The RR bands of Tyr in deoxy-Hb A were observed at 1618 (Y8a), 1208 (Y7a), 1178 (Y9a), and 853 cm^{-1} (Y1). The frequency downshifts of the Y8a and Y9a RR bands

dx.doi.org/10.1021/bi300347x | *Biochemistry* 2012, 51, 5932−5941

in the CO-form are distinctive. The RR bands of Trp in deoxy-Hb A were observed at 1557 (W3), 1360 and 1340 (W7, Trp doublet), 1011 (W16), 878 (W17), and 755 cm^{-1} (W18). The intensities of these Trp RR bands were appreciably reduced in the CO-form. The spectral changes of Tyr and Trp residues in Hb A due to the T → R transition (Figure 5B) are in good agreement with those reported previously.[8−11,13]

Figure 6 compares the deoxy-minus-CO difference spectra of α14Trp mutant (A), β15Trp mutant (B), and β37Trp mutant

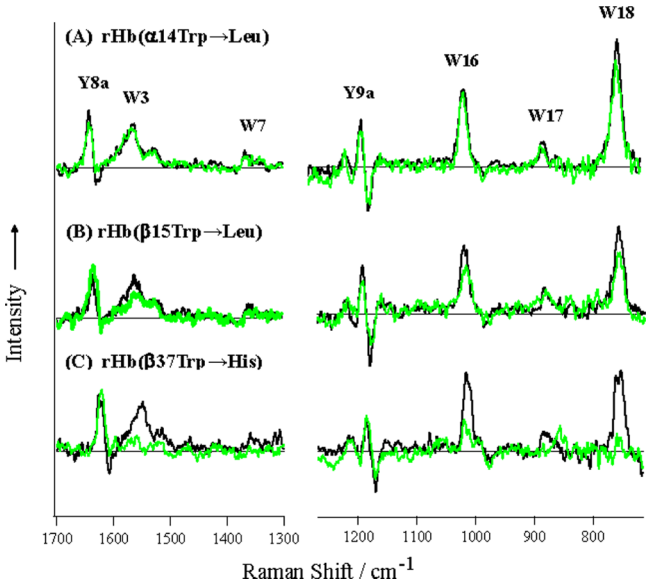

Figure 6. Comparison of deoxy-minus-CO difference UVRR spectra of Hb A (black spectra) with those of rHb(αW14L) (A), rHb(βW15L) (B), and rHb(βW37H) (C) (green spectra). The spectra of Hb A were measured under the same experimental conditions as those for each mutant Hb. Therefore, they are slightly different.

(C) (green spectra) with those of Hb A (black spectra). The difference spectra of Hb A are slightly different among spectra A, B, and C because they were measured under the experimental conditions same as those for individual mutant Hbs at the same time, but this indicates the reproducibility of the present experiments. The deoxy(T)-minus-CO(R) difference spectra excited at 229−235 nm contain prominent peaks assigned to both Tyr and Trp residues.[11,31−33] The characteristic R → T difference spectra exhibit frequency shifts for Tyr RR bands and intensity enhancements for Trp RR bands.[10,11] These UVRR spectral changes were attributed to conformational changes in the residues at the $\alpha1-\beta2$ subunit interface, especially β37Trp, β145Tyr, α140Tyr, and α42Tyr.[12,33] Among the three spectra (A, B, and C) shown in Figure 6, the spectral changes in Y8a and Y9a of Tyr are alike, indicating that changes in Tyr residues in the three mutant Hbs occur normally upon ligand binding. However, the intensity enhancements of Trp RR bands are different among the three mutants. Although the changes in Trp in rHb(αW14L) (Figure 6A) are the same as those of Hb A, those in rHb(βW15L) (Figure 6B) are slightly smaller, and those in rHb(βW37H) are markedly smaller than those of Hb A. A weak peak around 870 cm^{-1} in Figure 6C is due to noises. These results clearly indicate that the main changes in Trp RR bands for the R → T quaternary structure transition are due to β37Trp as suggested before,[10,11] but β15Trp also appreciably contributes to them.

The difference spectra between Hb A and each mutant Hb are expected to reflect the state of each Trp residue in Hb A. The UVRR spectra of each Trp residue are shown in Figure 7

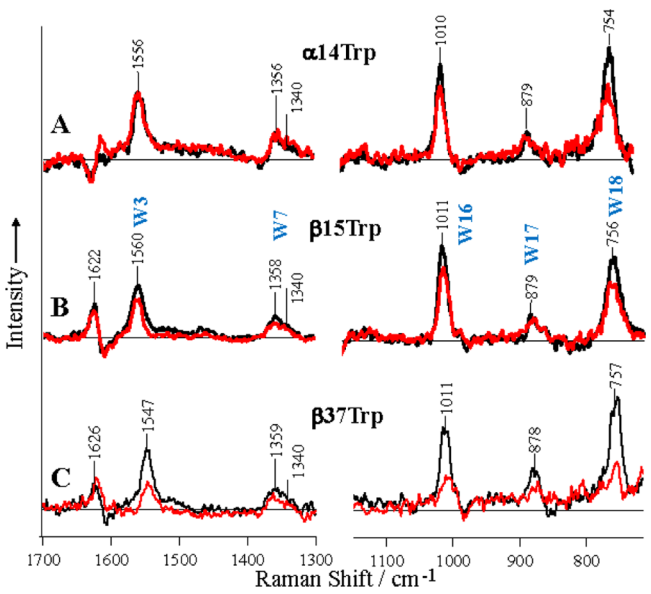

Figure 7. UVRR spectra of individual α14Trp (A), β15Trp (B), and β37Trp (C) in the CO-form (red spectra) and deoxy-form (black spectra). These spectra were digitally obtained by subtraction of the UVRR spectrum of each mutant Hb from that of Hb A in both the CO- and deoxy-forms, respectively.

for both CO-form (red spectra) and deoxy-form (black spectra). The W3 frequency of Trp, which is known to be sensitive to the absolute value of the torsion angle, $\chi^{2,1}$, about the C_2-C_3 bond connecting the indole ring to the peptide main chain,[30] was observed at 1556 cm^{-1} for α14Trp, 1560 cm^{-1} for β15Trp, and 1547 cm^{-1} for β37Trp. Their $\chi^{2,1}$ angles were deduced from the W3 frequencies on the basis of the correlation curve, which was determined empirically with the reported values of the $\chi^{2,1}$ angles of various Trp derivatives in a crystalline state and W3 frequencies.[30] From the correlation curve, the $\chi^{2,1}$ angles of each Trp residue in the deoxy mutant Hbs in solution are deduced to be 108° (α14Trp), 125° (β15Trp), and 87° (β37Trp). The X-ray structure of deoxy-Hb A indicated that the $\chi^{2.1}$ angles were 102° for α14Trp, 103° for β15Trp, and 93° for β37Trp.[13] These values from the crystal structure are slightly different from those inferred from the W3 frequencies for solutions. This might be due to structural differences between in crystal and solution states.

The W7 doublet of Trp at 1340 and 1360 cm^{-1} is known to reflect environmental hydrophobicity of the indole ring.[34] The band at 1360 cm^{-1} is more intense than that of 1340 cm^{-1} in a hydrophobic environment and is reversed in a hydrophilic environment.[34] The relative intensities (I_{1360}/I_{1340}) for α14Trp, β15Trp, and β37Trp in the deoxy-form are 3.0, 2.0, and 1.6, respectively (Figure 7), although these values are not precise due to band overlapping. For model compounds of Trp (indole and Nac-L-Trp EE), the range of the I_{1360}/I_{1340} ratio is known to be 0.65−0.92 for hydrophilic solvents and 1.23−1.32 for hydrophobic solvents.[34] From these facts, it is suggested that the three Trp residues in Hb A are all placed in a hydrophobic environment, but the α14Trp and β15Trp residues are placed in a more hydrophobic environment than the β37Trp residue.

dx.doi.org/10.1021/bi300347x | *Biochemistry* 2012, 51, 5932−5941

The frequency of the 878 cm^{-1} band (W17) is known to reflect the strength of hydrogen bond at the N_1H site of the indole ring. Indeed, the W17 band of skatole appears at 882−883 cm^{-1} in non-hydrogen-bonding solvents and 877−878 cm^{-1} in hydrogen-bonding solvents.[30] The W17 bands for α14Trp, β15Trp, and β37Trp appear at 879, 879, and 878 cm^{-1}, respectively (Figure 7). It is inferred from the frequencies of the three Trp residues that the N_1H sites of the indole ring of all Trp residues are hydrogen-bonded in deoxy-Hb A.

Although the spectrum of the α14Trp residue (Figure 7A) is almost the same between the deoxy- and CO-forms, that of the β15Trp residue (Figure 7B) is slightly different. In contrast, the Trp RR bands for the β37Trp residue in the CO-form were greatly reduced in intensity and slightly shifted (2−4 cm^{-1}) to lower frequencies (Figure 7C). A derivative-shaped feature at the Y8a position in the HbA-minus-α14Trp mutant difference spectrum (Figure 7A) is different from the shape of Y8a in the other difference spectra (Figure 7B,C). However, we thought that this is not due to structural alteration by α14Trp replacement but is caused by some noises in spectral subtraction because spectral changes of Tyr RR bands both at Y8a and Y9a are almost identical with those of Hb A as shown in Figure 6A.

Quaternary T Conformation of rHb(βW37H). X-ray crystallographic studies[1,2] have demonstrated the presence of two quaternary structures of Hb A: low-affinity (T) and high affinity (R) structures. Isolated chains of Hb A, Mb, and mutant Hbs with high oxygen affinity would adopt the R structure even in the deoxy-forms, and mutant Hbs with low oxygen affinity (Hb M Boston and Hb Kansas) would adopt the T structure even in the liganded form.[35] Sol−gel encapsulated Hb A binds and releases oxygen noncooperatively, as if the encapsulation limits ligand-induced quaternary structure change.[36,37] However, resonance Raman studies showed that encapsulation dramatically slows down but does not prevent the tertiary and quaternary structure changes.[38] UVRR difference spectra obtained have revealed that E-helix motion is initiated upon ligand binding, as indicated by the appearance of the W3 difference band for α14- and β15Trp at 1559 cm^{-1}.[39] The subsequent appearance of Tyr (Y8a and Y9a) and Trp (W3, 1549 cm^{-1}) bands in the UVRR difference spectra suggests conformational shifts for the penultimate α140Tyr on F-helix, α42Tyr in the "switch" region, and β37Trp in the "hinge" region.[39,40] Thus, two populations have been found for encapsulated T state and referred as "low-affinity T" and "high-affinity T" states.[41−44] The low-affinity T exhibits the same oxygen affinity as the ordinary T-state Hb A in crystal[45] and iron−zinc hybrid Hbs.[46] Upon ligand binding to the initial deoxy state structure under encapsulation, the low affinity-T population relaxes first, and later the high affinity-T population does along the same path.[42]

Noble et al.[47] and Kiger et al.[48] determined ligand binding properties of β37Trp mutants, βW37G, βW37A, βW37E, and βW37Y, and demonstrated that the substitution of β37Trp could destabilize the tetrameric form relative to their constituent dimers and also alter cooperativity of the intact tetrameric species. The functional alterations from wild-type are dependent on a side chain of the substituted residue, with varied magnitudes of change increasing as Trp is substituted by Tyr (Hill's n = 2.4), Ala (n = 1.4), Gly (n = 1.2), and Glu (n = 1.1). Crystallographic experiments of these mutant Hbs identify the structural transition referred as T-to-T_{high} between the quaternary T state of wild-type deoxyHb and an ensemble of related T-like quaternary structures observed for some mutations in the β37Trp cluster and/or by exposing crystals of wild-type or mutant Hbs to oxygen.[49] The T-to-T_{high} quaternary structure transitions consist of a rotation of the ($\alpha1\beta1$) dimer relative to ($\alpha2\beta2$) dimer as well as a coupled bending within the ($\alpha\beta$) dimer that practically involves a small rotation of the α1 subunit relative β1 subunit. Mutations of β37Trp disrupt quaternary constraints in the β37Trp cluster and result in the high-affinity structure referred as T_{high}. Oxygen binding properties of βW37H has not been reported so far, but crystallographic analysis was done.[49] According to their data (Table 2),[49] the disruption of quaternary structure is large for βW37E, βW37A, and βW37G but is small for βW37Y and βW37H, indicating that the quaternary T-structure of βW37Y and βW37H mutants with significant cooperativity (n > 2.0) seems to be close to that of wild-type deoxyHb A.

Table 2. Effects of Solvent Polarity on Absorption and CD Spectra of Nac-L-Trp EE[a]

solvent	relative polarity[b]	Abs(L_b)/nm	CD_{max}/nm	$\Delta\varepsilon$ (×10)
water	1.000	287.6	289	+ 0.50
methanol	0.762	289.4	289	+ 1.08
2-propanol	0.546	289.8	290	+ 0.58
chloroform	0.259	290.0	288	− 1.80
1,4-dioxane	0.164	290.4	286	− 2.05
diethyl ether	0.117	290.2	289	− 0.82
CCl_4	0.052	292.0	291	− 0.80

[a]Nac-L-Trp EE (1.1 mg) was dissolved in 5 mL of each solvent, and we examined absorption and near-CD spectra with a cell having a 2 mm light path length at 25 °C. Scan speed and data sampling of CD were 20 nm/min and 0.2 nm, respectively. Forty scans were averaged. [b]The values for relative polarity were extracted from: Reichardt, C. *Solvents and Solvent Effects in Organic Chemistry*, 3rd ed.; Wiley-VCH Publishers: Weinheim, 2003.

CD and UVRR Spectra of Model Compounds of Trp. Since the majority of Trp residues have no free amino and carboxyl groups in proteins, it seems that *N*-acetyl-L-tryptophan ethyl ester (Nac-L-Trp EE) is a useful model compound for Trp residues in proteins. The differences in the CD and UVRR spectra among the Trp residues in Hb A possibly reflect the differences in environmental hydrophobicity and/or the hydrogen bonding of Trp in a globin molecule. To check this possibility, the solvent effects on the CD and UVRR spectra of Trp were examined using a model compound of Trp, Nac-L-Trp EE.

Model Compounds for Trp. As shown in Figure S1, the absorption (a) and UVRR spectra (c) of Nac-L-Trp EE are almost the same as those of L-Trp. The absorption spectra (a) of Nac-L-Trp EE and L-Trp exhibited a broad peak in the 250−300 nm region, which is due to an overlapped band of the L_a (275−280 nm) and L_b (ca. 290 nm) transitions.[50,51] On the contrary, their CD spectra (b) are strikingly different from each other. The CD spectrum of Nac-L-Trp EE has distinct L_b bands at 289 and 283 nm superimposed with a weak L_a band at 270 nm, but that of L-Trp appears mainly from the L_a band at 267 nm, as shown before.[52,53] Indole-3-methyl (skatole), indole-3-acetic acid, and indole-3-pyruvic acid did not show any CD bands in the near-UV CD region, as shown in Figure S2 (right panel). On the other hand, these indole-3-derivatives displayed similar absorption (Figure S2, left panel) and UVRR spectra (Figure S3).

dx.doi.org/10.1021/bi300347x | *Biochemistry* 2012, 51, 5932−5941

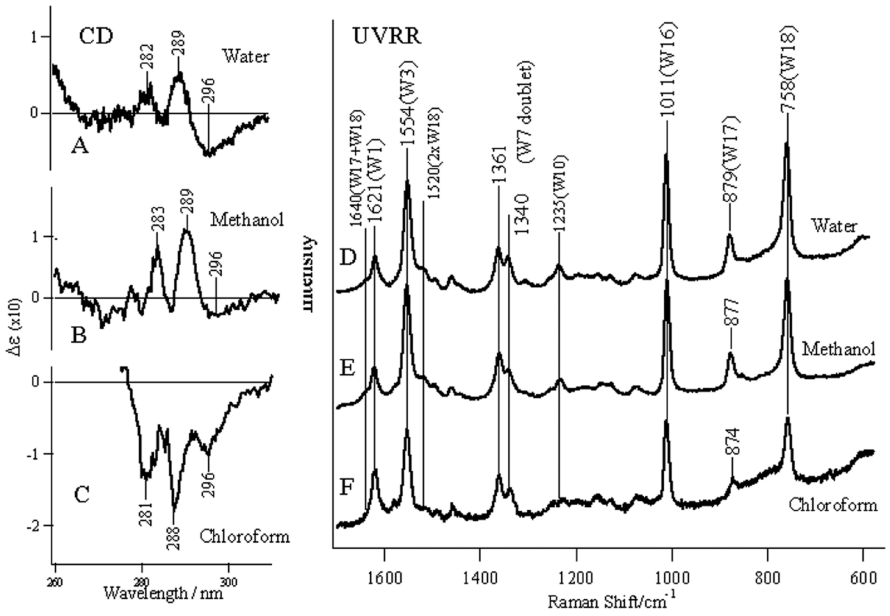

Figure 8. Solvent effects on near-UV CD (left panel) and UVRR (right panel) spectra of Nac-L-Trp EE. Nac-L-Trp EE (1.1 mg) was dissolved in 5 mL of solvent, and its CD spectrum was measured with a cell having a 2 mm light path length for every 0.2 nm of sampling with a scan speed of 20 nm/min. The spectra shown are an average of 40 scans. The 229 nm excited UVRR spectra are the sum of 60 exposures with each exposure accumulating for 30 s.

The absorption and UVRR spectra of these model compounds derive from the indole ring, but CD definitely originated from the asymmetry of the α-carbon. The α-carbon has no π electrons. Therefore, the π electronic states of the indole ring must be coupled with those of the amide groups through the asymmetric carbon. Since the coupling is associated with a magnetic dipole, the energy levels of π electrons of indole ring are hardly perturbed by the coupling, and therefore, the loss of asymmetric carbon in indole-3-derivatives scarcely affects the absorption and UVRR spectra but affects the CD spectra in the 250−300 nm region. This coupling must be sensitive to the electronic states of groups attached to the α-carbon. In fact, acetylation of the amino group and esterification of the carboxy group of L-Trp caused great changes in the near-UV CD spectrum, as shown in Figure S1b. It is highly possible that the near-UV CD spectrum of Trp reflects the electronic state of peptide groups connected with the α-carbon.

In the UVRR spectra of model compounds, however, there are also slight differences in the Fermi doublet (W7) among the four indole-3-derivatives. The Fermi doublet (W7) is observed at ∼1360 and ∼1340 cm^{-1} except for indole-3-methyl (skatole), which gives only one band at 1340 cm^{-1} (Figure S3). The Fermi doublet is considered to arise from Fermi resonance between the N_1C_8 stretching fundamental (W7) and the combination of out-of-plane deformation modes.[54] It is likely that the short side chain of skatole changed the frequencies of the out-of-plane deformation modes, and as a result the intensity borrowing of the combination mode ceased to occur.

Solvent Effects. The dependence of the CD spectra of Nac-L-Trp EE on relative polarity of solvents is summarized in Table 2. On going from water (hydrogen-bonding and hydrophilic) to a CCl_4 solution (non-hydrogen-bonding and hydrophobic), the L_b bands in the absorption spectrum were shifted to red by 4 nm but the L_a band scarcely changed (data not shown). On the other hand, a sign of ellipticity seems to have a relation with solvent hydrophobicity, but the wavelength yielding the maximum in the CD spectra has no correlation.

Figure 8 (left panel) shows CD spectra of Nac-L-Trp EE in water (A), methanol (B), and chloroform (C). In water and/or methanol, Nac-L-Trp EE exhibited positive CD bands at 282−283 and 289 nm. These positive CD bands were observed for solvents having relative polarity higher than 0.5. In contrast, Nac-L-Trp EE displayed negative CD bands in hydrophobic solvents, such as chloroform (Figure 8C), 1,4-dioxane (Figure 9, inset), diethyl ether (Table 2), and CCl_4 (Figure 10, right panel). Presumably, the peptide groups attached to the α-carbon of Nac-L-Trp EE are influenced by the relative polarity of the solvent. Here, we conclude that Trp residues in a protein give rise to positive or negative CD for the L_b bands in a

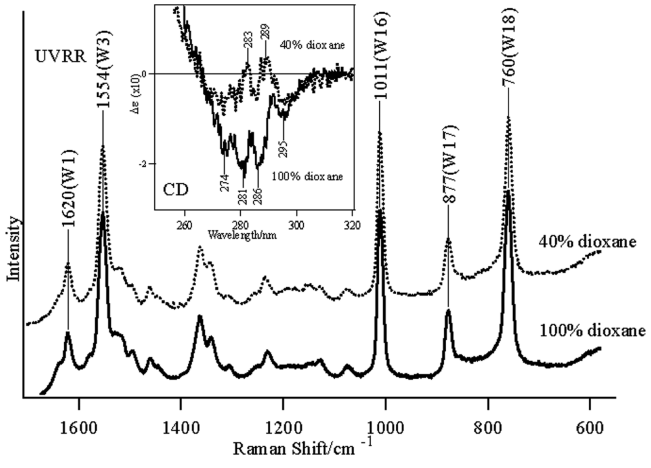

Figure 9. Effects of water addition on CD (inset figure) and UVRR spectra of Nac-L-Trp EE in 1,4-dioxane. Nac-L-Trp EE (1.1 mg) was dissolved in 5 mL of 100% 1,4-dioxane or 40% 1,4-dioxane (dioxane:water = 4:6). Measurements of the CD and UVRR spectra were carried out under the same conditions as those for Figure 8.

dx.doi.org/10.1021/bi300347x | *Biochemistry* 2012, 51, 5932−5941

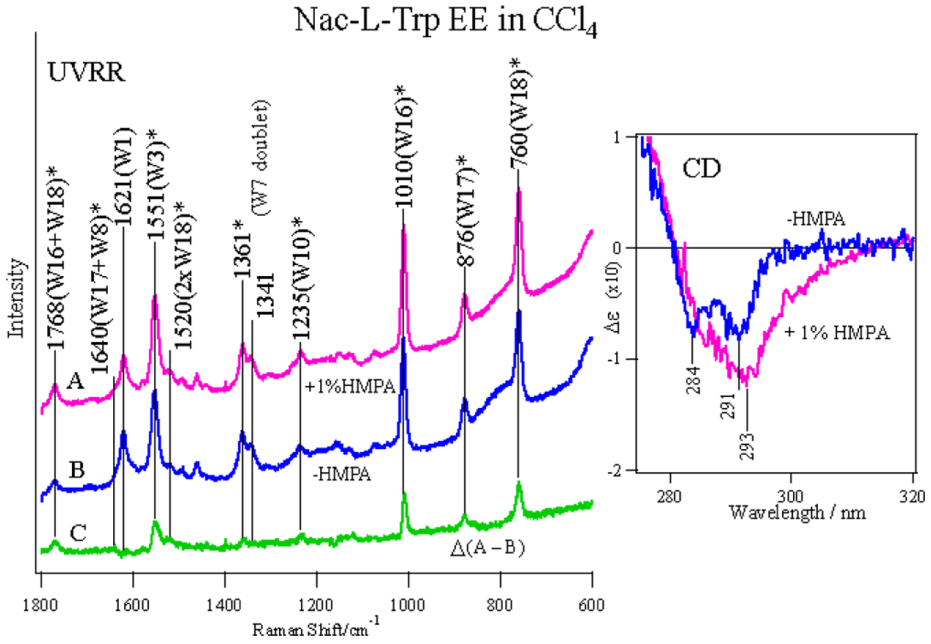

Figure 10. Effects of hydrogen-bonding at indole N_1H site of Nac-L-Trp EE on UVRR (left panel) and CD (right panel) spectra. Nac-L-Trp EE (1.1 mg) was dissolved in 5 mL of CCl_4, and its CD spectrum measured with a cell having a 2 mm light path length for every 0.2 nm of sampling with a scan speed of 20 nm/min with and without 1% HMPA. The spectra shown are an average of 100 scans. UVRR spectra with and without 1% HMPA were also measured with a sum of 60 exposures with each exposure accumulating for 30 s. Raman bands marked with an asterisk denote the band which changed upon the addition of HMPA.

hydrophilic or hydrophobic environment, respectively, through status changes of peptide groups attached to its α-carbon.

Figure 8 (right panel) shows the 229 nm excited UVRR spectra of Nac-L-Trp EE in the same solvents as for CD spectra (left panel). The relative peak intensities of W1, W3, W16, and W18 are different between the spectrum in chloroform (Figure 8F) and those in water (Figure 8D) and methanol (Figure 8E), although the frequencies of major Raman bands do not change, contrary to the remarkable changes in the CD spectra. However, it is noted that small but distinct differences were observed between the polar (water and methanol) and nonpolar solvents (chloroform) at 1640 (W17 + W18), 1520 (2 × W18), and 1235 cm^{-1} (W10). In addition, the intensity ratios of W1/W3 and W16/W18 are larger in chloroform than those in water and/or methanol. Recently, it was reported that the W10/W9 intensity ratio ($R_{W10} = I_{\sim1237(W10)}/I_{\sim1254(W9)}$) of Nac-L-Trp EE increases upon the formation of a hydrogen bond.[55]

Figure 9 compares the CD spectrum of Nac-L-Trp EE dissolved in a solution of 40% dioxane (dioxane:water = 4:6) with that in 100% dioxane. The absorption maximum at 290 nm of Nac-L-Trp EE in 100% dioxane shifts to 289 nm in 40%, and negative CD bands in 100% dioxane change toward positive in 40% dioxane, as shown in the inset. This result further supports the possibility that negative CD bands of Nac-L-Trp EE arise in a hydrophobic environment and change toward positive in a less hydrophobic environment. Figure 9 also shows the UVRR spectra of Nac-L-Trp EE in 100% and 40% dioxane. The relative intensity of W16 and W18 increases slightly, and the ratio of the W7 doublet changes from 1.5 in 100% dioxane to 1.3 in 40% dioxane, probably reflecting the surrounding hydrophobicity of the indole ring of Nac-L-Trp EE. However, the other Raman bands remain unchanged between 100% and 40% dioxane. Therefore, it became more evident that the CD spectrum of the L_b band reflects a state of peptide groups attached to the α-carbon of Trp rather than a state of the indole ring itself.

Hydrogen Bonding. It is known that the UVRR bands exhibit high intensity when the indole N_1H site is hydrogen-bonded with a proton acceptor in hydrophobic environments.[56] To separate the effects of hydrogen-bonding of Nac-L-Trp EE on CD and UVRR spectra from those of hydrophobic environments, we used hexamethylphosphoric triamide (HMPA), a strong hydrogen bonding acceptor.[56,57]

Figure 10 (left panel) shows the UVRR spectra of Nac-L-Trp EE in CCl_4 with (A) and without (B) 1% HMPA (v/v against CCl_4) and the difference spectrum (C) between them (A − B). The positive peaks in the difference spectrum (C) indicate that the intensity increases of the Raman bands upon hydrogen-bond formation at N_1H. This difference spectrum is similar to the deoxy-minus-CO difference spectrum shown in Figure 5B except the UVRR bands of Tyr, indicating that a part of the T-to-R quaternary structure transition of Hb A is due to hydrogen-bonding at N_1H of β37Trp. Furthermore, a positive peak in the difference spectrum for W10 supports the note of Schlamadinger et al. that the W10/W9 intensity ratio ($R_{W10} = I_{\sim1237(W10)}/I_{\sim1254(W9)}$) increases upon the formation of a hydrogen bond.[55] On account of this hydrogen bond, the negative CD band at 284 nm of Nac-L-Trp EE decreased in intensity and the negative band at 291 nm shifted to a longer wavelength and intensified, as shown by Figure 10 (right panel). Thus, in the CD spectra, the hydrogen-bonding effects can be distinguished from the surrounding polarity effects shown in Figure 8A–C. The CD changes in β37Trp upon deoxygenation of Hb A (Figure 4C) probably reflect the hydrogen-bond formation in the deoxy-form. These changes in UVRR and near-UV CD spectra of Nac-L-Trp EE in CCl_4 with HMPA were not observed for its dioxane solution, as shown in Figure S4.

dx.doi.org/10.1021/bi300347x | *Biochemistry* 2012, 51, 5932–5941

■ ASSOCIATED CONTENT

Supporting Information

Absorption, CD and UVRR spectra of L-Trp, Nac-L-Trp EE, and indole-3-derivatives, and the effect of HMPA on UVRR and CD spectra of Nac-L-Trp EE in 1,4-dioxane. This material is available free of charge via the Internet at http://pubs.acs.org.

■ AUTHOR INFORMATION

Corresponding Author

*Tel +81-42-387-5120, Fax +81-42-387-5121, e-mail masako.nagai.gv@hosei.ac.jp (M.N.); Tel +81-791-58-0323, Fax +81-791-58-0323, e-mail teizo@sci.u-hyogo.ac.jp (T.K.).

Funding

This work was supported in part by the Global COE Program, "Picobiology: Life Science at the Atomic Level" at the Graduate School of Life Science, University of Hyogo, from MEXT, Japan (to T.K.), by MEXT-Supported Program for the Strategic Research Foundation at Private Universities, 2008-2012, Japan (to K.I.) and by Grants-in-aid for Scientific Research from the Ministry of Education, Culture, Science, Sports, and Technology of Japan to K.I. (22570217) and T.K. (24350086).

Notes

The authors declare no competing financial interest.

■ ACKNOWLEDGMENTS

We thank Professor Chien Ho of Carnegie Melon University for the gift of the *E. coli* Hb expression plasmid, pHE7, and Dr. Yayoi Aki of Kanazawa University for constructing plasmids and expressing mutant Hbs.

■ ABBREVIATIONS

CD, circular dichroism; CO, carbon monoxide; Hb, hemoglobin; Hb A, human adult Hb; HMPA, hexamethylphosphoric triamide; IHP, inositol hexaphosphate; Nac-L-Trp EE, *N*-acetyl-L-tryptophan ethyl ester; OEC, oxygen equilibrium curve; R, relaxed; rHb, recombinant Hb; T, tense; Trp, tryptophan; Tyr, tyrosine; UVRR, ultraviolet resonance Raman.

■ REFERENCES

(1) Perutz, M. F. (1970) Stereochemistry of cooperative effects in haemoglobin. *Nature 228*, 726−739.

(2) Perutz, M. F. (1979) Regulation of oxygen affinity of hemoglobin: influence of structure of the globin on the heme iron. *Annu. Rev. Biochem. 48*, 327−386.

(3) Fung, L. W., and Ho, C. (1975) A proton nuclear magnetic resonance study of the quaternary structure of human hemoglobins in water. *Biochemistry 14*, 2526−2535.

(4) Simon, S. R., and Cantor, C. R. (1969) Measurement of ligand-induced conformational changes in hemoglobin by circular dichroism. *Proc. Natl. Acad. Sci. U. S. A. 63*, 205−212.

(5) Perutz, M. F., Ladner, J. E., Simon, S. R., and Ho, C. (1974) Influence of globin structure on the state of the heme. I. Human deoxyhemoglobin. *Biochemistry 13*, 2163−2173.

(6) Jin, Y., Sakurai, H., Nagai, Y., and Nagai, M. (2004) Changes of near-UV CD spectrum of human hemoglobin upon oxygen binding: A study of mutants at α42, α140, β145 tyrosine or β37 tryptophan. *Biopolymers 74*, 60−63.

(7) Aki-Jin, Y., Nagai, Y., Imai, K., and Nagai, M. (2007) Changes of near-UV circular dichroism spectra of human hemoglobin upon the R → T quaternary structure transition, in *New Approarches in Biomedical Spectroscopy*, ACS Symposium Series 963 (Kneipp, K., Aroca, R., Kneipp, H., and Wentrup-Byrne, E., Eds.) pp 297−311, American Chemical Society, Washington, DC.

(8) Huang, S., Peterson, E. S., Ho, C., and Friedman, J. M. (1997) Quaternary structure sensitive tyrosine interactions in hemoglobin: A UV resonance Raman study of the double mutant rHb (β99Asp→Asn, α42Tyr→Asp). *Biochemistry 36*, 6197−6206.

(9) Rodgers, K. R., and Spiro, T. G. (1994) Nanosecond dynamics of the R → T transition in hemoglobin: ultraviolet Raman studies. *Science 265*, 1697−1699.

(10) Rodgers, K. R., Su, C., Subramaniam, S., and Spiro, T. G. (1992) Hemoglobin R→T structural dynamics from simultaneous monitoring of tyrosine and tryptophan time-resolved UV resonance Raman signals. *J. Am. Chem. Soc. 114*, 3697−3709.

(11) Nagai, M., Kaminaka, S., Ohba, Y., Nagai, Y., Mizutani, Y., and Kitagawa, T. (1995) Ultraviolet resonance Raman studies of quaternary structure of hemoglobin using a tryptophan β37 mutant. *J. Biol. Chem. 270*, 1636−1642.

(12) Nagai, M., Wajcman, H., Lahary, A., Nakatsukasa, T., Nagatomo, S., and Kitagawa, T. (1999) Quaternary structure sensitive tyrosine residues in human hemoglobin: UV resonance Raman studies of mutants at α140, β35, and β145 tyrosine. *Biochemistry 38*, 1243−1251.

(13) Hu, X., and Spiro, T. G. (1997) Tyrosine and tryptophan structure markers in hemoglobin ultraviolet resonance Raman spectra: mode assignments via subunit-specific isotope labeling of recombinant protein. *Biochemistry 36*, 15701−15712.

(14) Dickerson, R. E., and Geis, I. (1983) in *Hemoglobin: Structure, Function, Evolution, and Pathology*, Benjamin/Cummings, Menlo Park, CA.

(15) Fermi, G., Perutz, M. F., Shaanan, B., and Fourme, R. (1984) The crystal structure of human deoxyhaemoglobin at 1.74 Å resolution. *J. Mol. Biol. 175*, 159−174.

(16) Baldwin, J., and Chothia, C. (1979) Haemoglobin: the structural changes related to ligand binding and its allosteric mechanism. *J. Mol. Biol. 129*, 175−220.

(17) Shen, T. J., Ho, N. T., Zou, M., Sun, D. P., Cottam, P. F., Simplaceanu, V., Tam, M. F., Bell, D. A., Jr., and Ho, C. (1997) Production of human normal adult and fetal hemoglobins in *Escherichia coli*. *Protein Eng. 10*, 1085−1097.

(18) Chen, Z., and Ruffner, D. E. (1998) Amplification of closed circular DNA *in vitro*. *Nucleic Acids Res. 26*, 1126−1127.

(19) Nagai, M., Nagai, Y., Aki, Y., Imai, K., Wada, Y., Nagatomo, S., and Yamamoto, Y. (2008) Effect of reversed heme orientation on circular dichroism and cooperative oxygen binding of human adult hemoglobin. *Biochemistry 47*, 517−525.

(20) Imai, K. (1982) *Allosteric Effects in Haemoglobin*, Cambridge University Press, London.

(21) Adair, G. S. (1925) The hemoglobin system. VI. The oxygen dissociation curve of hemoglobin. *J. Biol. Chem. 63*, 529−545.

(22) Imai, K. (1981) Analysis of ligand binding equilibria. *Methods Enzymol. 76*, 470−486.

(23) Hayashi, A., Suzuki, T., and Shin, M. (1973) An enzymic reduction system for metmyoglobin and methemoglobin, and its application to functional studies of oxygen carriers. *Biochim. Biophys. Acta 310*, 309−316.

(24) Lynch, R. E., Lee, R., and Cartwright, G. E. (1976) Inhibition by superoxide dismutase of methemoglobin formation from oxyhemoglobin. *J. Biol. Chem. 251*, 1015−1019.

(25) Winterboum, C. C., McGrath, B. M., and Carrell, R. W. (1976) Reactions involving superoxide and normal and unstable haemoglobins. *Biochem. J. 155*, 493−502.

(26) Dudik, J. M., Johnson, C. R., and Asher, S. A. (1985) Wavelength dependence of the preresonance Raman cross sections of CH_3CN, SO_4^{2-}, ClO_4^-, and NO_3^-. *J. Chem. Phys. 82*, 1732−1740.

(27) Arisaka, F., Nagai, Y., and Nagai, M. (2011) Dimer-tetramer association equilibria of human adult hemoglobin and its mutants as observed by analytical ultracentrifugation. *Methods 54*, 175−180.

(28) Hsu, M.-C., and Woody, R. W. (1969) Origin of the rotational strength of heme transitions in myoglobin. *J. Am. Chem. Soc. 91*, 3679−3681.

(29) Miura, T., Takeuchi, H., and Harada, I. (1988) Characterization of individual tryptophan side chains in proteins using Raman

spectroscopy and hydrogen-deuterium exchange kinetics. *Biochemistry 27*, 88−94.
(30) Miura, T., Takeuchi, H., and Harada, I. (1989) Tryptophan Raman bands sensitive to hydrogen bonding and side-chain conformation. *J. Raman Spectrosc. 20*, 667−671.
(31) Nagatomo, S., Nagai, M., and Kitagawa, T. (2011) A new way to understand quaternary structure changes of hemoglobin upon ligand binding on the basis of UV-resonance Raman evaluation of intersubunit interactions. *J. Am. Chem. Soc. 133*, 10101−10110.
(32) Jayaraman, V., Rodgers, K. R., Mukerji, I., and Spiro, T. G. (1995) Hemoglobin allostery: resonance Raman spectroscopy of kinetic intermediates. *Science 269*, 1843−1848.
(33) Nagai, M., Imai, K., Kaminaka, S., Mizutani, Y., and Kitagawa, T. (1996) Ultraviolet resonance Raman studies of hemoglobin quaternary structure using a tyrosine-α42 mutant: changes in the $\alpha_1\beta_2$ subunit interface upon the T → R transition. *J. Mol. Struct. 379*, 65−75.
(34) Harada, I., Miura, T., and Takeuchi, H. (1986) Origin of the doublet at 1360 cm^{-1} and 1340 cm^{-1} in the Raman spectra of tryptophan and related compounds. *Spectrochim. Acta, Part A 42*, 307−308.
(35) Fermi, G., and Perutz, M. F. (1981) in *Atlas of Molecular Structures in Biology, 2. Haemoglobin & Myoglobin* (Fillips, D. C., and Richards, F. M., Eds.) Clarendon Press, Oxford.
(36) Shibayama, N., and Saigo, S. (1995) Fixation of the quaternary structures of human adult haemoglobin by encapsulation in transparent porous silica gels. *J. Mol. Biol. 251*, 203−209.
(37) Bettati, S., and Mozzarelli, A. (1997) T state hemoglobin binds oxygen noncooperatively with allosteric effects of protons, inositol haxaphosphate, and chloride. *J. Biol. Chem. 272*, 32050−32055.
(38) Das, T. K., Khan, I., Rousseau, D. L., and Friedman, J. M. (1999) Temperature dependent quaternary state relaxation in sol-gel encapsulated hemoglobin. *Biospectroscopy 5*, S64−70.
(39) Juszczak, L. J., and Friedman, J. M. (1999) UV resonance Raman spectra of ligand binding intermediates of sol-gel encapsulated hemoglobin. *J. Biol. Chem. 274*, 30357−30360.
(40) Kavanaugh, J. S., Rogers, P. H., Arnone, A., Hui, H. L., Wierzba, A., DeYoung, A., Kwiatkowski, L. D., Noble, R. W., Juszczak, L. J., Peterson, E. S., and Friedman, J. M. (2005) Intersubunit interactions associated with Tyr42α stabilize the quaternary-T tetramer but are not major quaternary constraints in deoxyhemoglobins. *Biochemistry 44*, 3806−3820.
(41) Juszczak, L., Samuni, U., and Friedman, J. M. (2005) Conformational and functional significance of the α140 side-chain in HbA: a UV and visible resonance Raman study of three α140 mutants. *J. Raman Spectrosc. 36*, 350−358.
(42) Samuni, U., Dantsker, D., Juszczak, L. J., Bettati, S., Ronda, L., Mozzarelli, A., and Friedman, J. M. (2004) Spectroscopic and functional characterization of T state hemoglobin conformations encapsulated in silica gels. *Biochemistry 43*, 13674−13682.
(43) Bruno, S., Bonaccio, M., Bettati, S., Rivetti, C., Viappiani, C., Abbruzzetti, S., and Mozzarelli, A. (2001) High and low oxygen affinity conformations of T state hemoglobin. *Protein Sci. 10*, 2401−2407.
(44) Samuni, U., Roche, C. J., Dantsker, D., Juszczak, L. J., and Friedman, J. M. (2006) Modulation of reactivity and conformation within the T-quaternary states of human hemoglobin: The combined use of mutagenesis and sol-gel encapsulation. *Biochemistry 45*, 2820−2835.
(45) Rivetti, C., Mozzarelli, A., Rossi, G. L., Henry, E. R., and Eaton, W. A. (1993) Oxygen binding by single crystals of hemoglobin. *Biochemistry 32*, 2888−2906.
(46) Samuni, U., Juszczak, L., Dantsker, D., Khan, I., Friedman, A. J., Perez-Gonzalez-de-Apodaca, J., Bruno, S., Hui, H. L., Colby, J. E., Karasik, E., Kwiatkowski, L. D., Mozzarelli, A., Noble, R., and Friedman, J. M. (2003) Functional and spectroscopic characterization of half-liganded iron-zinc hybrid hemoglobin: Evidence for conformational plasticity within the T-state. *Biochemistry 42*, 8272−8288.
(47) Noble, R. W., Hui, H. L., Kwiatkowski, L. D., Paily, P., DeYoung, A., Wierzba, A., Colby, J. E., Bruno, S., and Mozzarelli, A. (2001) Mutational effects at the subunit interfaces of human hemoglobin: Evidence for a unique sensitivity of the T quaternary state to changes in the hinge region of the $\alpha1\beta2$ interface. *Biochemistry 40*, 12357−12368.
(48) Kiger, L., Klinger, A. L., Kwiatkowski, L. D., De Young, A., Doyle, M. L., Holt, J. M., Noble, R. W., and Ackers, G. K. (1998) Thermodynamic studies on the equilibrium properties of a series of recombinant βW37 hemoglobin mutants. *Biochemistry 37*, 4336−4345.
(49) Kavanaugh, J. S., Rogers, P. H., and Arnone, A. (2005) Crystallographic evidence for a new ensemble of ligand-induced allosteric transitions in hemoglobin: The T-to-T_{high} quaternary transitions. *Biochemistry 44*, 6101−6121.
(50) Stickland, E. H., Horwitz, J., and Billups, C. (1970) Near-ultraviolet absorption bands of tryptophan. Studies using indole and 3-methylindole as models. *Biochemistry 9*, 4914−4921.
(51) Stickland, E. H., Billups, C., and Kay, E. (1972) Effects of hydrogen bonding and solvents upon the tryptophanyl ^{1}La absorption band. Studies using 2,3-dimethylindole. *Biochemistry 11*, 3657−3662.
(52) Stickland, E. H., Horwitz, J., and Billups, C. (1969) Fine structure in the near-ultraviolet circular dichroism and absorption spectra of tryptophan derivatives and chymotripsinogen A at 77 K. *Biochemistry 8*, 3205−3213.
(53) Stickland, E. H., and Beychok, S. (1974) Aromatic contributions to circular dichroism spectra of proteins. *CRC Crit. Rev. Biochem. 2*, 113−175.
(54) Dieng, S. D., and Schelvis, J. P. M. (2010) Analysis of measured and calculated Raman spectra of indole, 3-methylindole, and tryptophan on the basis of observed and predicted isotope shifts. *J. Phys. Chem. A 114*, 10897−10905.
(55) Schlamadinger, D. E., Gable, J. E., and Kim, J. E. (2009) Hydrogen bonding and solvent polarity markers in the UV resonance Raman spectrum of tryptophan: Application to membrane proteins. *J. Phys. Chem. B 113*, 14769−14778.
(56) Matsuno, M., and Takeuchi, H. (1998) Effects of hydrogen bonding and hydrophobic interactions on the ultraviolet resonance Raman intensities of indole ring vibrations. *Bull. Chem. Soc. Jpn. 71*, 851−857.
(57) Kamlet, M. J., and Taft, R. W. (1976) The solvatochromic comparison method. I. The β-scale of solvent hydrogen-bond acceptor (HBA) basicities. *J. Am. Chem. Soc. 98*, 377−383.